DELPHI Collaboration

DELPHI 2001-012 CONF 453
2 February 2001

Update of the search for supersymmetric particles in light gravitino scenarios at $\sqrt{s}$ from 204 to 208 GeV

**R. Alemany[1], E. Anashkin[2], F. Cavallo[3], P. Checchia[2], C. García[4],
F. Navarria[3], F. Mazzucato[5], E. Piotto[1], U. Schwickerath[1]**

Abstract

An update of the search for sleptons, sgoldstinos and heavy stable charged particles is presented in the context of light gravitino scenarios. Data collected in 2000 with the DELPHI detector at centre-of-mass energies from 204 to 208 GeV were analysed. No evidence for the production of these supersymmetric particles was found. Hence, new mass limits were derived at 95% confidence level.

Paper submitted to the Moriond Conference 2001

[1] CERN, CH-1211 Geneva 23, Switzerland,

[2] INFN, Via Marzolo 8, 35131 Padova, Italy,

[3] INFN, Viale Berti-Pichat 6/2, 40127 Bologna, Italy,

[4] IFIC, Avda. Dr. Molliner 50, Burjassot 46100, Valencia, Spain,

[5] Geneva University, Quai Ernest-Ansermet 24, CH-1211 Geneva 4, Switzerland.

1 Introduction

In 2000 the centre-of-mass energies reached by LEP ranged from 204 GeV to 208 GeV, and the DELPHI experiment collected an integrated luminosity of 223.53 pb^{-1}. The data were analysed to update the searches for sleptons, sgoldstinos and heavy stable charged particles in the context of Gauge Mediated Supersymmetry Breaking (GMSB) models [1, 2].

Once Supersymmetry is spontaneously broken, the gravitino ($\tilde{G}$) can acquire a mass by absorbing the degrees of freedom of the goldstino [3]. In GMSB models $\tilde{G}$ is the lightest supersymmetric particle (LSP) and the next-to-lightest supersymmetric particle (NLSP) can be either the neutralino ($\tilde{\chi}_1^0$) or the sleptons ($\tilde{l}$) [4]. In the search for sleptons, the data were analysed under the assumption that the NLSP is a slepton, and in particular two scenarios were considered, the $\tilde{\tau}_1$ NLSP ($\tilde{\tau}_1^\pm \to \tau^\pm \tilde{G}$) and the sleptons co-NLSP ($\tilde{l}_R^\pm \to l^\pm \tilde{G}$) scenarios.

Due to the coupling of the NLSP to $\tilde{G}$, the mean decay length ($\hat{L}$) of the former can range from micrometres to metres depending on the mass of the gravitino ($m_{\tilde{G}}$):

$$\hat{L} = 1.76 \times 10^{-3} \sqrt{\left(\frac{E_{\tilde{l}}}{m_{\tilde{l}}}\right)^2 - 1} \left(\frac{m_{\tilde{l}}}{100\,\text{GeV}/c^2}\right)^{-5} \left(\frac{m_{\tilde{G}}}{1\,\text{eV}/c^2}\right)^2 \quad cm \qquad (1)$$

For example, for $m_{\tilde{G}} \lesssim 250$ eV/c^2, or equivalently, for a SUSY breaking scale of $\sqrt{F} \lesssim 1000$ TeV (since both parameters are related [5]), the decay of a NLSP with mass greater than for example 60 GeV/c^2 can take place within the detector. This range of $\sqrt{F}$ is in fact consistent with astrophysical and cosmological considerations [6].

The first search presented in the note concerns $\tilde{l}$ pair production followed by the decay of each slepton into a lepton and a gravitino:

$$e^+ e^- \to \tilde{l}^+ \tilde{l}^- \to l^+ \tilde{G} l^- \tilde{G} \qquad (2)$$

If the decay length is too short (1 eV/$c^2 \lesssim m_{\tilde{G}} \lesssim 10$ eV/c^2) to allow the reconstruction of the slepton, only the corresponding lepton or its decay products will be seen in the detector, and the search will then be based on the track impact parameter. If the slepton decays inside the tracking devices (10 eV/$c^2 \lesssim m_{\tilde{G}} \lesssim 1000$ eV/c^2), the signature will be at least one track of a charged particle with a kink or a decay vertex. However, for very heavy gravitinos ($m_{\tilde{G}} \gtrsim 1000$ eV/c^2), the decay length is large and the slepton decays outside the detector. The pair production of such long-lived or stable particles yields a characteristic signature with typically two back-to-back charged heavy objects in the detector. Finally, for very light gravitino masses ($m_{\tilde{G}} \lesssim 1$ eV/c^2), the decay takes place in the primary vertex and the results from the search for sleptons in gravity mediated (MSUGRA) models can be applied.

Heavy stable charged particles are predicted not only in GMSB models but also in Minimal Supersymmetric Standard Models (MSSM) with a very small amount of R-parity violation, or with R-parity conservation if the mass difference between the LSP and the NLSP becomes very small. In these models the LSP can be a charged slepton or a squark and decay with a long lifetime into Standard Model particles [7]. The typical signature of these events are two massive particles traversing the detector which do not produce Cherenkov radiation in DELPHI's Ring Imaging CHerenkov (RICH) detectors, but high ionization losses in the Time Projection Chamber. Updated lower mass limits on heavy

stable charged particles, under the assumption that the LSP is a charged slepton, will be provided in this note within both models, GMSB and MSSM.

Recently it has been pointed out [8] that an appropriate theory must contain also the supersymmetric partner of the goldstino called sgoldstino which could be massive. In the minimal R-parity conserving model, as considered in [8], the effective theory at the weak scale contains two neutral scalar states: S, CP-even and P, CP-odd (from now on the two states will be labelled with the generic symbol ϕ since the discussion applies to both of them). It must be pointed out that sgoldstinos have R-even parity, therefore they are not necessarily produced in pairs and their decay chains do not necessarily contain an LSP. The production of these particles may be relevant at LEP2 energies in light gravitino scenarios. One of the most interesting production channels is the process $e^+e^- \to \phi\gamma$ which depends on the ϕ mass (m_ϕ) and on $\sqrt{F}$. The most relevant ϕ decay modes are $\phi \to \gamma\gamma$ and $\phi \to gg$. The corresponding branching ratios depend on the gaugino masses M_1, M_2 and M_3, and the total width is $\Gamma \sim \Gamma(\phi \to \gamma\gamma) + \Gamma(\phi \to gg)$. In this note two sets for these parameters as suggested in [8] are considered and listed in Table 1.

	M_1	M_2	M_3	$BR(\phi \to \gamma\gamma)$	$BR(\phi \to gg)$
1)	200	300	400	4%	96%
2)	350	350	350	11%	89%

Table 1: Two choices for the gaugino mass parameters (in GeV/c^2) relevant for the sgoldstino production and decay, and the corresponding branching ratios (BR) of the two considered channels.

The total width for a large interval of the parameter space is narrow (below a few GeV/c^2), except for the region with small $\sqrt{F}$ where also the production cross section is expected to be very large. The two considered decay channels produce events with very different topologies. The channel $\phi \to \gamma\gamma$ gives events with three high energy photons, one of which with energy $E_\gamma = \frac{s - m_\phi^2}{2\sqrt{s}}$ for the large fraction of the parameter space where ϕ has a negligible width. Despite the lower ϕ decay branching ratio (4 and 11% for the two sets of Table 1, respectively), this final state is worth investigating because the main background source is the QED $e^+e^- \to \gamma\gamma(\gamma)$ process, which is expected to be small if photons in the forward region are discarded. On the other hand, the channel $S \to gg$ gives events with one monochromatic photon (except for the region with small $\sqrt{F}$) and two jets. An irreducible background from $e^+e^- \to q\bar{q}\gamma$ events is associated to this topology and therefore the signal must be searched for as an excess of events over the background expectations for every mass hypothesis.

The data samples are described in section 2. The efficiencies of the different selection criteria and the number of events selected in data and in the Standard Model (SM) background are reported in 3. Finally, the results are presented in section 4.

2   Data sample and event generators

The analysis is based on data collected with the DELPHI detector during 2000 at centre-of-mass energies from 204 to 208 GeV. The total integrated luminosity analysed is 223.53 pb^{-1}. A detailed description of the DELPHI detector can be found in [9] and the detector performance in [10].

To evaluate the signal efficiencies and background contamination, events were generated using different programs, all relying on `JETSET 7.4` [11], tuned to LEP 1 data [12] for quark fragmentation.

Slepton pair samples at 208 GeV centre-of-mass energy were produced with `PYTHIA 5.7`[11] with staus having a mean decay length from 0.25 to 200 cm and masses from 60 to 104 GeV/c^2.

Other samples of slepton pairs were produced with at 206 and 208 GeV with `SUSYGEN` [13] for the small impact parameter search with $m_{\tilde{\tau}}$ from 90 GeV/c^2 to 102 GeV/c^2, and $m_{\tilde{\mu}}$ equal to 90 GeV/c^2 .

For the search for heavy stable charged particles, signal efficiencies were estimated from pair produced heavy smuons, generated at energies of 205 GeV and 206.7 GeV and 208 GeV with `SUSYGEN`. The events were passed through the detector simulation as heavy muons. The efficiencies were estimated for masses between 10 GeV/c^2 and 100 GeV/c^2 (1000 events were generated per mass point).

For the sgoldstino search, signal efficiencies were estimated from samples obtained as explained in [14].

The background process $e^+e^- \rightarrow q\bar{q}(n\gamma)$ was generated with `PYTHIA 6.125`, while `KORALZ 4.2` [15] was used for $\mu^+\mu^-(\gamma)$ and $\tau^+\tau^-(\gamma)$. The generator `BHWIDE` [16] was used for $e^+e^- \rightarrow e^+e^-$ events.

Processes leading to four-fermion final states were generated using `EXCALIBUR 1.08` [17] and `GRC4F` [18].

Two-photon interactions leading to hadronic final states were generated using `TWOGAM` [19], including the VDM, QPM and QCD components. The generators of Berends, Daverveldt and Kleiss [20] were used for the leptonic final states.

The cosmic radiation background was studied using the data collected before the beginning of the 2000 LEP run.

The generated signal and background events were passed through the detailed simulation [10] of the DELPHI detector and then processed with the same reconstruction and analysis programs used for real data.

3 Data selection

3.1 Slepton pair production

This section describes the update of the search for slepton pair production as a function of the mean decay length. The details of the selection criteria used to search for the topologies obtained when the NLSP decays inside the detector volume were described in [21, 22]. The efficiencies were derived for different $\tilde{l}$ masses and decay lengths by applying the same selection to the simulated signal events.

3.1.1 Search for secondary vertices

This analysis exploits a feature of the $\tilde{l} \rightarrow l\tilde{G}$ topology when the slepton decays inside the tracking devices, namely, one or two tracks originating from the interaction point and at least one of them with a secondary vertex or a kink.

The secondary vertex reconstruction procedure was sensitive to radial decay lengths (R) between 20 cm and 90 cm. The Vertex detector and the Inner detector were needed

to reconstruct the $\tilde{\tau}$ and the Time Projection Chamber to reconstruct the decay products. The shape of the efficiency distribution was quite flat as a function of R decreasing when the $\tilde{\tau}$ decayed near the outer surface of the Time Projection Chamber. The decrease was due to inefficiencies in the reconstruction of the tracks coming from the decay products of the τ. Figure 1-a shows the efficiency distribution as a function of the decay radius for $\tilde{\tau}$ masses between 60 and 90 GeV/c^2 and $\hat{L} = 50$ cm. The same selection criteria were applied to smuons and selectrons. The efficiency, within the same range of decay radius, was around 60% (40%) for $m_{\tilde{\mu}_R}$ ($m_{\tilde{e}_R}$) between 60 to 90 GeV/c^2. The efficiency for selectrons was lower than for staus or smuons due to an upper cut on total electromagnetic energy at the preselection level.

After applying the selection criteria to search for this topology, two events in real data were found to satisfy all the requirements, while $0.94^{+1.12}_{-0.28}$ were expected from SM backgrounds.

3.1.2 Large impact parameter search

To investigate the region of lower gravitino masses the previous search was extended to the case of sleptons with mean decay length between 0.25 cm and approximately 10 cm. In this case the $\tilde{l}$ is not reconstructed and only the l (or the decay products in the case of $\tilde{\tau}$) is detected. The impact parameter search was applied to those events accepted by the same general requirements as in the search for secondary vertices, and not selected by the secondary vertex analysis.

The maximum efficiency was around 32% corresponding to a mean decay length of 2.5 cm. The efficiency decreased sharply for lower decay lengths due to the requirement on minimum impact parameter. For longer decay lengths, the appearance of reconstructed $\tilde{\tau}$ in combination with the cut on the maximum number of charged particles in the event caused the efficiency to decrease smoothly. This decrease is compensated by a rising efficiency in the search for secondary vertices. For masses above 60 GeV/c^2 no dependence on the $\tilde{\tau}$ mass was found far from the kinematic limit.

The same selection was applied to smuons and selectrons. For smuons the efficiency increased to $\sim 58\%$ for a mean decay length of 2.5 cm and masses over 60 GeV/c^2 since the smuon always has a one-prong decay. For selectrons the efficiency was $\sim 33\%$ for the same mean decay length and range of masses. Figure 1-b shows the efficiency distribution as a function of the mean decay length for staus, smuons and selectrons. The contribution of the kink and large impact parameter searches is shown.

Trigger efficiencies were studied simulating the DELPHI trigger response to the events selected by the vertex search and by the large impact parameter analysis, and were found to be around 99%.

Two events in the real data sample were selected, while $2.40^{+1.49}_{-0.45}$ were expected from SM backgrounds.

3.1.3 Small impact parameter search

The large impact parameter search can be extended further to mean decay lengths below 0.1 cm. The integrated luminosity used in this search is 164.5 pb^{-1} between 204 and 208 GeV center-of-mass energies. The analysis is essentially the same as described in detail in previous publications [21, 22], with the addition of the tightening of the cut on the

4

quality of the fastest track. The filter has been applied to the search for long lived $\tilde{\tau}$ and $\tilde{\mu}$. The impact parameters, b_1 and b_2, of the two leading tracks in low multiplicity events are used to discriminate against the SM background. Requiring $\sqrt{b_1^2 + b_2^2} \geq 600~\mu$m the efficiency depends little on the slepton mass and it can be parameterized as a function of the slepton decay length in the laboratory system. The efficiency for $\tilde{\tau}$ detection reaches $\sim 40\%$ for decay lengths around 2 cm, is still 16% for a decay length of 0.1 cm, and 13% for 20 cm. The efficiency for $\tilde{\mu}$ detection reaches 45% around 2 cm, 15% at 0.1 cm, and 17% at 20 cm.

With this selection the number of expected SM background events is 3.3 ± 0.3, and the number of candidates in the data is 4, compatible with the expected SM background.

3.1.4 Heavy Stable Charged particles search

The analysis described in [21, 23] has been applied to the data taken during 2000. The data set has been subdivided into 3 energy bins, corresponding to energies below 206 GeV ($85~\text{pb}^{-1}$), between 206 GeV and 207 GeV ($124~\text{pb}^{-1}$), and above 207 GeV ($11.4~\text{pb}^{-1}$). A careful run selection ensured that the RICH detectors were fully operational because the method used to identify heavy stable particles relies on the lack of Cherenkov radiation in DELPHI's RICH detectors. Signal efficiencies were estimated from Monte Carlo by simulating heavy sleptons with `SUSYGEN` and passing them through the detector simulation as heavy muons. The total background of 0.25 ± 0.04 events was estimated from data itself by counting the number of tracks passing the individual selection criteria. Only events with two or three charged particles were considered. Events were selected, if they contained at least one charged particle with:

1. a momentum above 5 GeV/c, a high ionization loss and no photons in the gas radiator were associated to the particle (gas veto) or,

2. a momentum above 15 GeV/c, an ionization loss at least 0.3 below the expectation for a proton and surviving the gas veto or,

3. a momentum above 15 GeV/c, surviving the gas and the liquid RICH veto.

An event was also selected if both event hemispheres contained particles with both either a high ionization loss or a gas veto, or both having a low ionization loss. Special care has been taken about the dE/dx in sector 6 (S6) of the Time Projection Chamber which died during the second half of data taking, reducing the efficiency of the search by several percent as the dE/dx search windows could not be applied to tracks pointing to S6. To recover some sensitivity for tracks pointing to S6, only the double veto search window was applied, requiring hits in the Vertex Detector, Inner Detector and Outer Detector to ensure a good propagation of the tracks through the RICH.

No candidate events were selected in data. Figure 2 show the data and the three main search windows. The expectation for a 90 GeV/c^2 mass signal is also shown. For particle masses below 60 GeV/c^2 the signal efficiencies are of the order of 30% and rise with increasing mass to about 76-78%. Then the efficiency drops when approaching the kinematical limit due to saturation effects, and it is assumed to be zero at the kinematical limit.

3.2 Sgoldstino search

3.2.1 $\phi \to \gamma\gamma$ channel

The selection criteria applied in the search for $\gamma\gamma\gamma$ topologies were the same reported in [14] where all the selection cuts are optimized to find three high energy photons one of them monochromatic.

No significant variation in the polar acceptance for a $\phi\gamma$ signal and in the selection efficiency inside the acceptance region were observed in the 2000 data with respect to previous values: polar acceptance=$(51 \pm 2)\%$ and efficiency = $(76.6 \pm 2.5)\%$. As explained in [14], the polar acceptance was evaluated by generating 4-vectors corresponding to the prompt photon and to the ϕ decay products, and applying the following polar cut: $42° < \theta < 89°$ (High Projection Chamber acceptance), and $25° < \theta < 32.4°$ (Forward Electromagnetic Calorimeter acceptance). As in [14], the photon energies are determined with a good precision from their measured directions and the energy resolution was evaluated by means of the QED background events generated according to [24]. This energy resolution was found to be better than 0.5% in the whole photon energy range, as in the previous years. The photon recoil mass spectra obtained for the events collected during 2000 run and for all the events including those reported in [14] are shown in Figure 3-a. The data are superimposed on the expected QED background distribution.

The number of selected events in data and the expected SM background are 22 and $20.3^{+1.5}_{-1.9}$, respectively. No significant background was found except for the QED contribution.

3.2.2 $\phi \to gg$ channel

This channel is expected to give rise to a final state with one monochromatic photon and two jets. Similarly to the $\gamma\gamma\gamma$ selection, no significant variation in the polar acceptance for a $\phi\gamma$ signal and in the selection efficiency inside the acceptance region were observed in the 2000 data with respect to the previous values: the acceptance is $(76 \pm 2)\%$ and the efficiency ranged from 20 to 55 % depending on the photon energy. The energy resolution was also unchanged. The photon recoil mass spectra obtained for the events collected during 2000 and previous years are shown in Figure 3-b. The data are superimposed on the expected SM background distributions.

The number of selected events in data and the expected SM background are 766 and 775 ± 5, respectively.

4 Results and interpretation

Since there was no evidence for a signal above the expected SM background, the number of candidates in data and the expected number of background events were used to set limits at the 95% confidence level (CL) on the pair production cross-section and masses of the sparticles searched for. The limits presented here are at $\sqrt{s} = 208$ GeV after combining the results of the searches at lower centre-of-mass energies with the likelihood ratio method [25].

4.1   Slepton pair production

The results of the search for slepton pair production are presented in the $(m_{\tilde{G}}, m_{\tilde{l}})$ plane combining the impact parameter, the secondary vertex and the stable heavy lepton analyses, and using all DELPHI data from 130 GeV to 208 GeV centre-of-mass energies.

The $\tilde{\tau}_1$ pair production cross-section depends on the mixing in the stau sector. There-fore, in order to put limits on the $\tilde{\tau}_1$ mass the mixing angle had to be fixed. The results presented here corresponds to a mixing angle in the stau sector which gives the minimum $\tilde{\tau}_1$ pair production cross-section and at the same time maintains $m_{\tilde{\tau}_1}^2 > 0$, Figure 4-a. Within the $\tilde{\tau}_1$ NLSP scenario, the impact parameter and secondary vertex analyses ex-tended the limit $m_{\tilde{\tau}_R} > 82.2$ GeV/c^2 for $m_{\tilde{G}} \lesssim 1$ eV/c^2, set by MSUGRA searches, up to $m_{\tilde{G}} = 400$ eV/c^2, reaching the maximum excluded value of $m_{\tilde{\tau}_R} = 93$ GeV/c^2 for $m_{\tilde{G}} = 130$ eV/c^2. For $m_{\tilde{G}} > 130$ eV/c^2 the best lower mass limit was set by the stable heavy lepton search.

Within the sleptons co-NLSP scenario, the cross-section limits were used to derive lower limits for $\tilde{l}_R$ (Figure 4-b) masses at 95% CL. Assuming mass degeneracy between the sleptons, these searches extended the limit $\tilde{l}_R > 89$ GeV/c^2 set by MSUGRA searches for very short NLSP lifetimes, up to $m_{\tilde{G}} = 700$ eV/c^2. For the MSUGRA case no lepton combination exists, so the best limit from the $\tilde{\mu}_R$ has been used. The maximum excluded value of $m_{\tilde{l}_R} = 96.5$ GeV/c^2 was achieved for $m_{\tilde{G}} = 150$ eV/c^2. For $m_{\tilde{G}} > 150$ eV/c^2 the best lower mass limit was set by the stable heavy lepton search. $\tilde{l}_R$ masses below 35 GeV/c^2 were excluded by LEP 1 data [26]. In the case of $\tilde{l}_R$ degeneracy, this limit improved to 41 GeV/c^2.

4.2   Heavy stable charged particle pair production

The results presented in section 3.1.4 were combined with previous DELPHI results in this channel, and cross-section limits were derived as indicated in Figure 5. From the intersection points with the predicted cross-sections for smuon or staus in the MSSM, left(right) handed smuons and staus can be excluded up to masses of 94.0(93.5) GeV/c^2 at 95% CL. No limits are given on selectrons here, because the cross-section can be highly suppressed by an additional t-channel sneutrino exchange contribution.

4.3   Sgoldstino production

No excess of events nor clear evidence of an anomalous production of events with monochromatic photons is observed in either of the channels. Therefore a limit on the cross-section of the new physics reaction contributing to the two topologies was set.

Since the expected ϕ branching ratio and total width depend on the mass parameters as explained in [8], the 95% CL cross-section limit was computed as a function of m_ϕ and $\sqrt{F}$ for the two sets of parameters listed in Table 1, and is shown in Figure 6. By comparing the experimental limits with the expected production cross-section, it is possible to determine a 95% CL excluded region on the parameter space as shown in Figure 7. As explained in [8], to keep the particle interpretation the total width Γ must be much smaller than m_ϕ and therefore the region with $\Gamma > 0.5 \times m_\phi$ was not considered.

5 Summary

Sleptons, sgoldstinos and heavy stable charged particles were searched for in the context of light gravitino models. In the case of sleptons two possibilities were explored: the $\tilde{\tau}_1$ NLSP and the sleptons co-NLSP scenarios. In the case of heavy stable charged particles results within the MSSM interpretation are also given.

No evidence for signal production was found in any of the searches. Hence, the DELPHI collaboration sets lower limits at 95% CL for the mass of the particles searched for.

References

[1] M. Dine, W. Fischler and M. Srednicki, Nucl. Phys. **B189** (1981) 575;
S. Dimopoulos and S. Raby, Nucl. Phys. **B192** (1981) 353;
M. Dine and W. Fischler, Phys. Lett. **B110** (1982) 227;
M. Dine and M. Srednicki, Nucl. Phys. **B202** (1982) 238;
L. Alvarez-Gaumé, M. Claudson and M. Wise, Nucl. Phys. **B207** (1982) 96;
C. Nappi and B. Ovrut, Phys. Lett. **B113** (1982) 175.

[2] M. Dine and W. Fischler, Nucl. Phys. **B204** (1982) 346;
S. Dimopoulos and S. Raby, Nucl. Phys. **B219** (1983) 479.

[3] S. P. Martin, hep-ph/9709356.

[4] K. Cheung, D. A. Dicus, B. Dutta, S. Nandi, Phys. Rev. **D58** (1998) 015008.
G. F. Giudice, R. Rattazzi, Phys. Rep. 322 (1999) 419.

[5] S. Deser and B. Zumino, *Phys. Rev. Lett.* **38** (1977) 1433;
E. Cremmer et al., *Phys. Lett.* **B 79** (1978) 231.

[6] S. Dimopoulos, M. Dine, S. Raby, S. Thomas and J. D. Wells, Nucl. Phys. Proc. Suppl. **A52** (1997) 38.
E. Calzetta, A. Kandus, F. D. Mazzitelli and C. E. M. Wagner, Phys. Lett. **B472** (2000) 287.

[7] H. Dreiner, hep-ph/9707435.

[8] E. Perazzi, G. Ridolfi and F. Zwirner, Nucl. Phys. **B574** (2000) 3.

[9] DELPHI Collaboration, P. Aarnio *et al.*, Nucl. Instr. and Meth. **303** (1991) 233.

[10] DELPHI Collaboration, P. Abreu *et al.*, Nucl. Instr. and Meth. **378** (1996) 57.

[11] T. Sjöstrand, Comp. Phys. Comm. **39** (1986) 347;
T. Sjöstrand, PYTHIA 5.6 *and* JETSET 7.3, CERN-TH/6488-92.

[12] DELPHI Collaboration, P. Abreu *et al.*, Z. Phys. **C73** (1996) 11.

[13] SUSYGEN 2.20, S. Katsanevas and S. Melachroinos in *Physics at LEP2*, CERN 96-01, **Vol. 2**, p. 328 and http://lyoinfo.in2p3.fr/susygen/susygen.html;
S. Katsanevas and P. Moravitz, Comp. Phys. Comm. **122** (1998) 227.

[14] DELPHI collab., P. Abreu et al., Phys. Lett. **B494** (2000) 203.

[15] S. Jadach, B.F.L. Ward and Z. Was, Comp. Phys. Comm. **79** (1994) 503.

[16] S. Jadach, W. Placzek, B.F.L. Ward, Phys. Lett. **B390** (1997) 298.

[17] F.A. Berends, R. Pittau, R. Kleiss, Comp. Phys. Comm. **85** (1995) 437.

[18] J. Fujimoto *et al.*, Comp. Phys. Comm. **100** (1997) 128.

[19] S. Nova, A. Olshevski, and T. Todorov, CERN Report 96-01, Vol. 2, p 224.

[20] F.A. Berends, P.H. Daverveldt, R. Kleiss, Comp. Phys. Comm. **40** (1986) 271,
Comp. Phys. Comm. **40** (1986) 285, Comp. Phys. Comm. **40** (1986) 309.

[21] DELPHI Collaboration, P. Abreu *et al.*, EP 2001-011 (Accepted by Phys.Lett.B).

[22] DELPHI Collaboration, P. Abreu *et al.*, Eur. Phys. J. **C16** (2000) 211.
DELPHI Collaboration, P. Abreu *et al.*, Eur. Phys. J. **C7** (1999) 595.
DELPHI Collaboration, P. Abreu *et al.*, Eur. Phys. J. **C6** (1999) 385.

[23] DELPHI Collaboration, P. Abreu *et al.*, Phys. Lett. **B478** (2000) 65.

[24] F.A. Berends and R. Kleiss, Nucl. Phys. **B186** (1981) 22.

[25] A.L. Read, *Modified Frequentist Analysis of Search Results (The CLs Method)*, CERN
2000-205.

[26] Particle Data Group, Eur. Phys. J. **C15** (2000) 1.
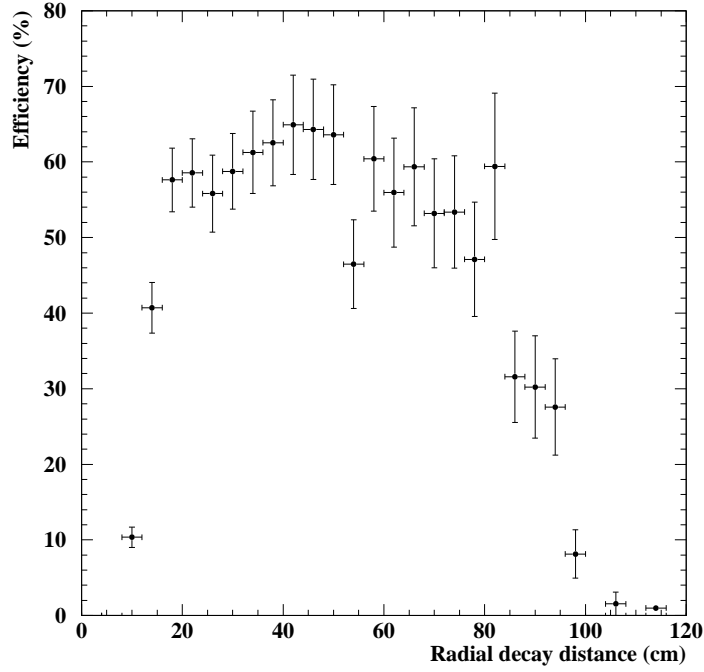
a)
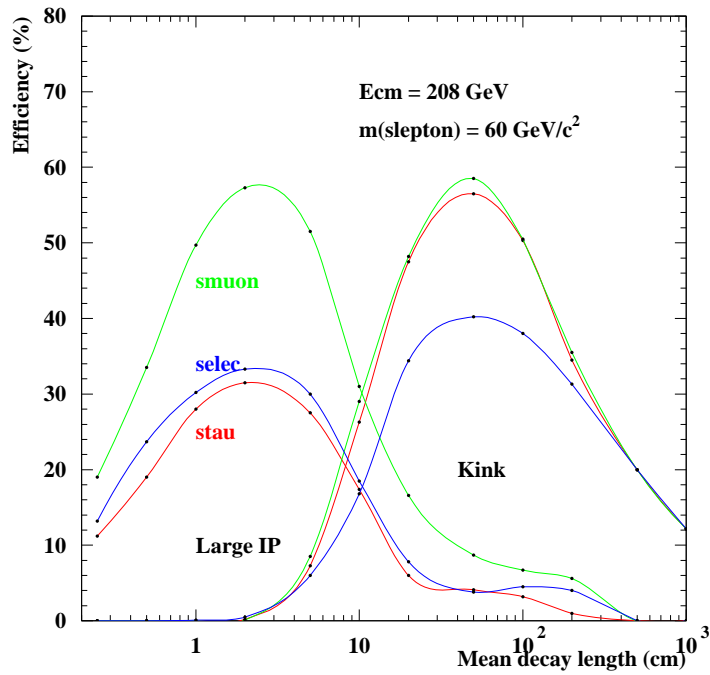
b)

Figure 1: a) Efficiency distribution as a function of the radial decay distance for staus with masses between 60 and 90 GeV/c^2 and $\hat{L} = 50$ cm and $\sqrt{s} = 208$ GeV. b) Efficiency distribution as a function of the mean decay length for staus, smuons and selectrons. The contribution of the kink and large impact parameter search is shown.
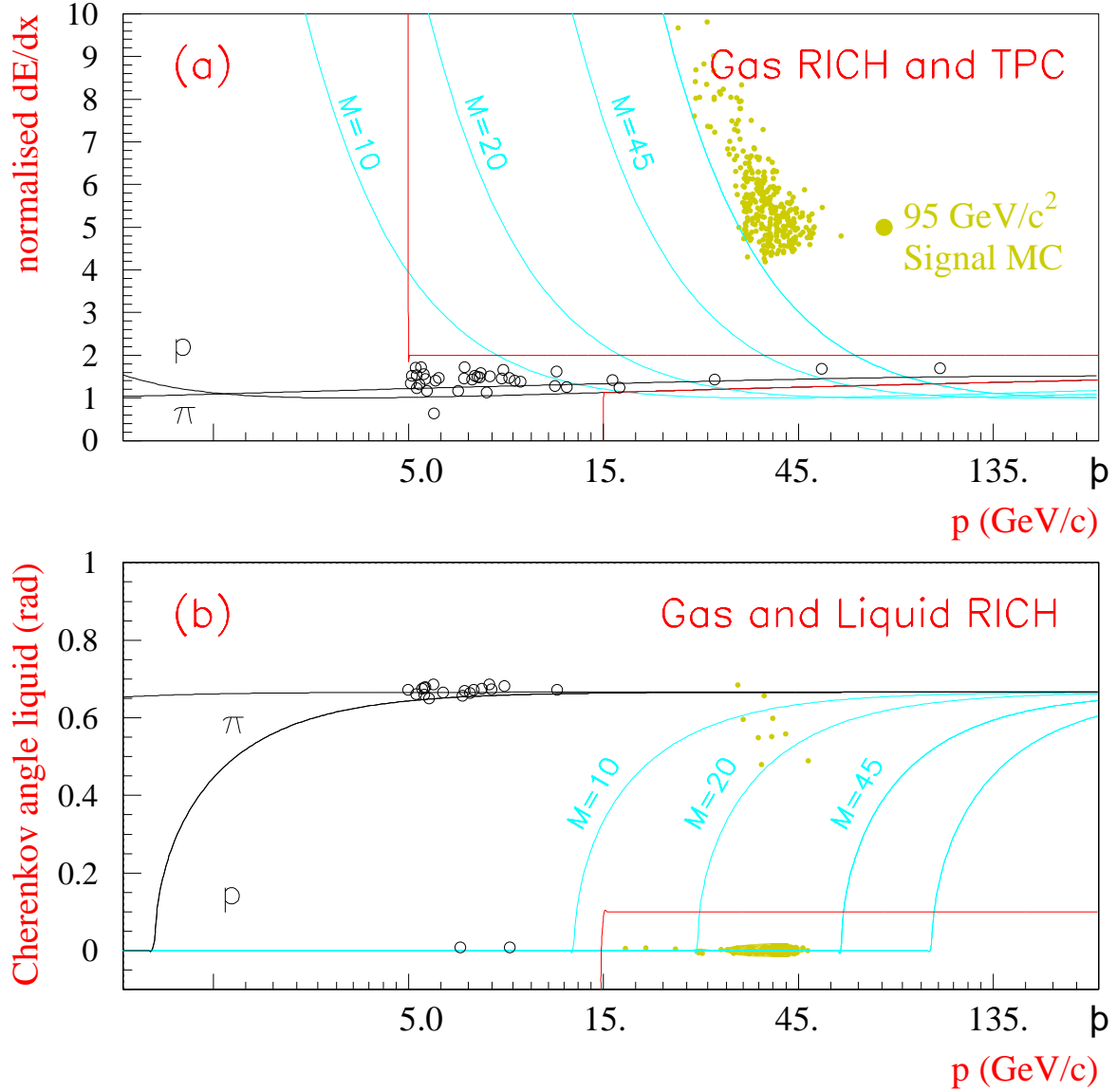
Figure 2: (a) Normalised energy loss as a function of the momentum after the gas veto for the 208 GeV data. (b) Measured Cherenkov angle in the liquid radiator as a function of the momentum after the gas veto: if four photons or less were observed in the liquid radiator, the Cherenkov angle was set equal to zero. The rectangular areas in (a) indicate selections (1) and (2), and that in (b) shows selection (3). The selection criteria are explained in the text. Open circles are data. The small filled circles indicate the expectation for a 90 GeV/c^2 mass signal with charge ±e, resulting in a large dE/dx (upper plot) and no photons (except for a few accidental rings) in the liquid Cherenkov counter (lower plot). The solid lines with a mass signal value indicate the expectation for heavy stable sleptons.
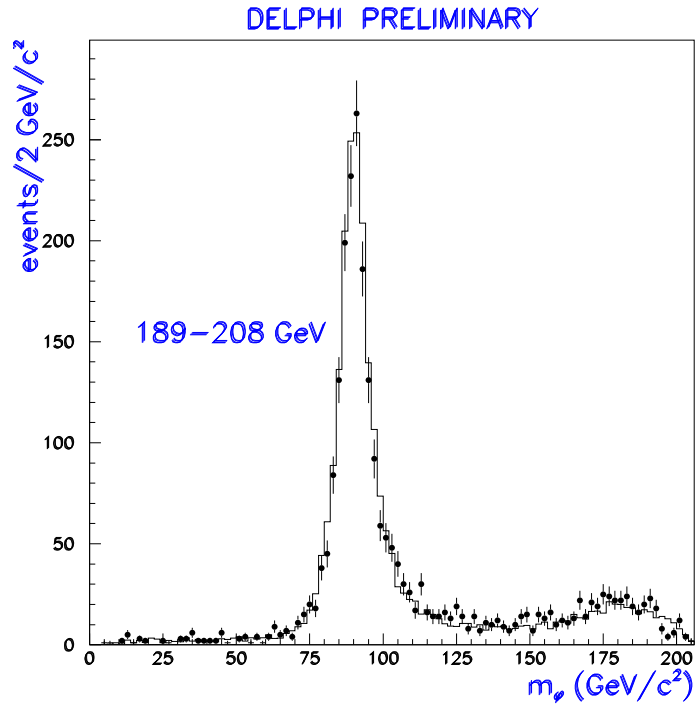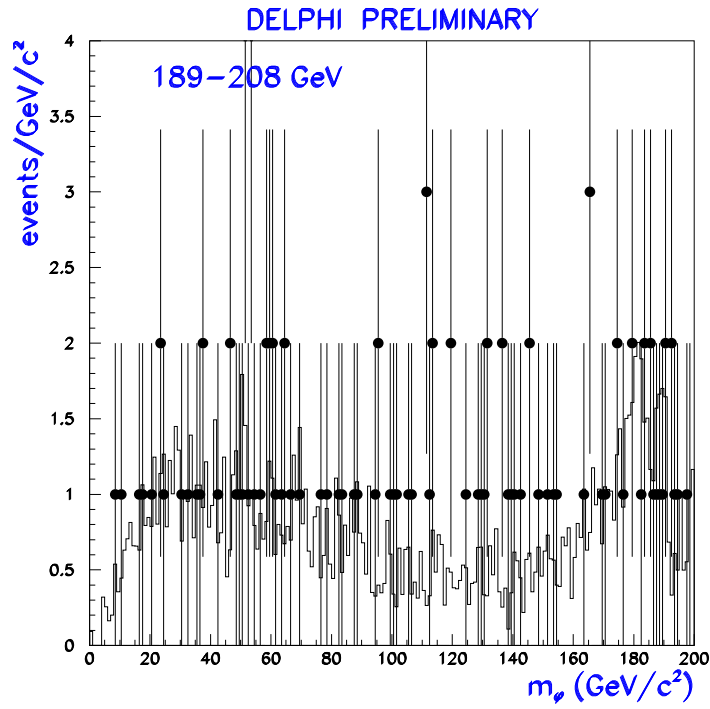
Figure 3: a) Photon recoil mass spectrum for $\gamma\gamma\gamma$ candidates (points) and the expected background (histogram). The average number of entries per event in the data is 2.3. The bin size takes into account the experimental mass resolution and the expected signal width. b) Photon recoil mass spectrum for γgg candidates (points) and the expected background (histogram).
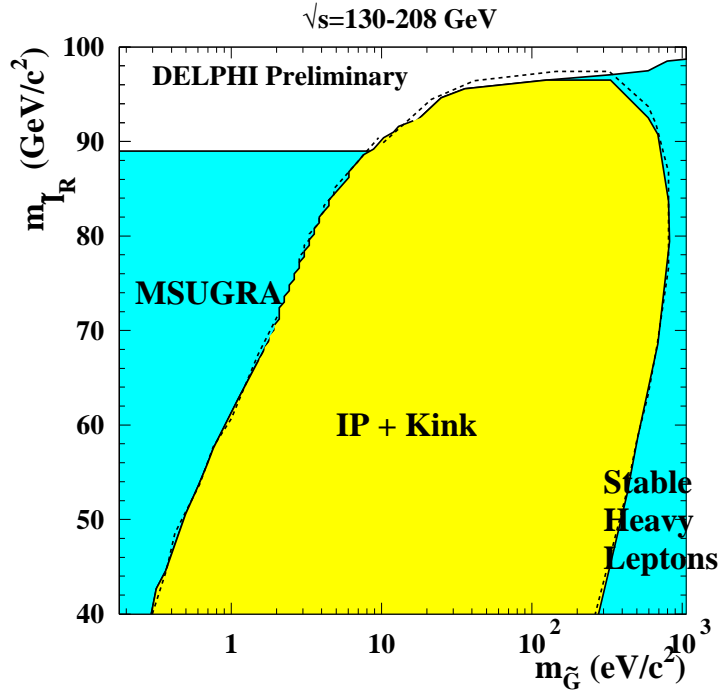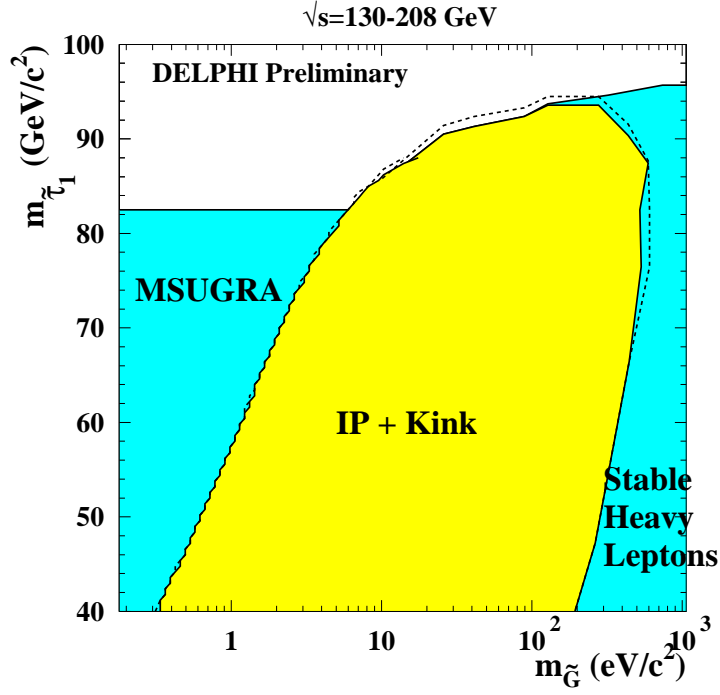
Figure 4: Exclusion regions in the $(m_{\tilde{G}}, m_{\tilde{\tau}_1})$ (a) and $(m_{\tilde{G}}, m_{\tilde{l}_R})$ (b) planes at 95% CL for the present analyses combined with the Stable Heavy Lepton search and the search for $\tilde{l}$ in gravity mediated models (MSUGRA), using all DELPHI data from 130 GeV to 208 GeV centre-of-mass energies. The dashed line shows the expected limits for the impact parameter and kink searches.
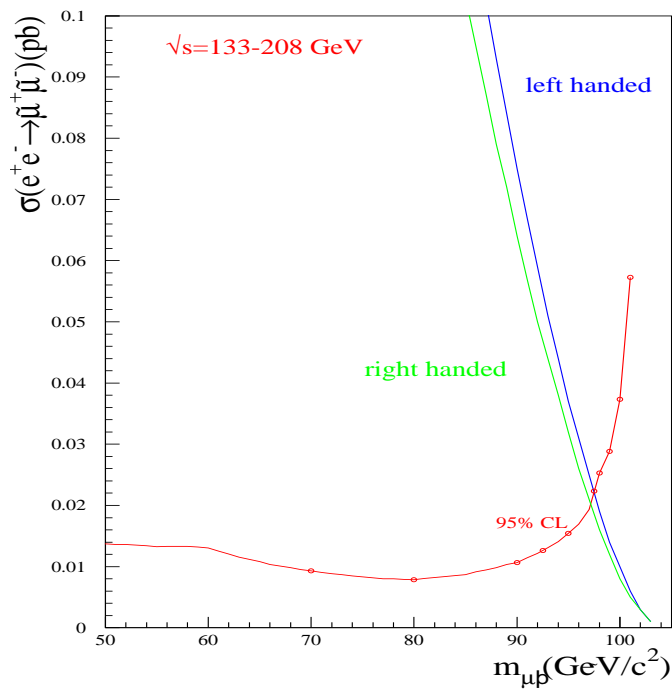
Figure 5: Predicted production cross-section for left and right handed stable smuons (staus) as a function of the particle mass. The cross-section limit indicated in the figure has been derived using all DELPHI data between 130 and 208 GeV.
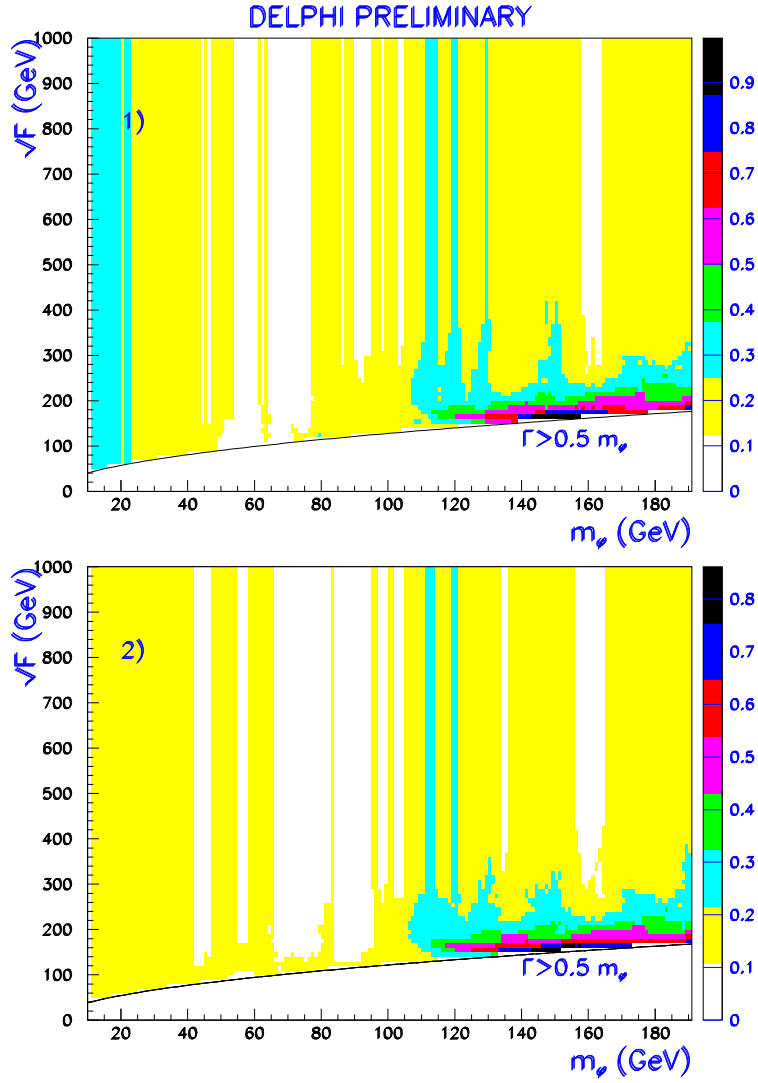
Figure 6: Cross section (pb) limit at the 95% Confidence Level as a function of m_ϕ and $\sqrt{F}$ for the two sets of parameters of Table 1 and using all DELPHI data between 189 and 208 GeV.
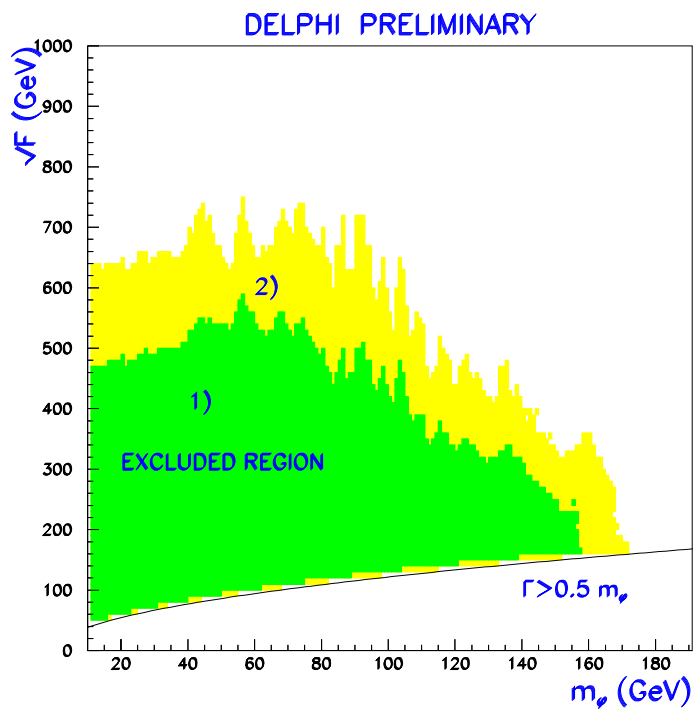
Figure 7: Exclusion region at the 95% Confidence Level in m_ϕ, $\sqrt{F}$ plane for the two sets of parameters of Table 1 and using all DELPHI data between 189 and 208 GeV.